Radio Science Investigations of the Saturn System with Voyager 1: Preliminary Results

Abstract. *Voyager 1 radio occultation measurements of Titan's equatorial atmosphere successfully probed to the surface, which is provisionally placed at a radius of 2570 kilometers. Derived scale heights plus other experimental and theoretical results indicate that molecular nitrogen is the predominant atmospheric constituent. The surface pressure and temperature appear to be about 1.6 bars and 93 K, respectively. The main clouds are probably methane ice, although some condensation of nitrogen cannot be ruled out. Solar abundance arguments suggest and the measurements allow large quantities of surface methane near its triple-point temperature, so that the three phases of methane could play roles in the atmosphere and on the surface of Titan similar to those of water on Earth. Radio occultation measurements of Saturn's atmosphere near 75° south latitude reached a maximum pressure of 1.4 bars, where the temperature is about 156 K. The minimum temperature is about 91 K near the 60-millibar pressure level. The measured part of the polar ionosphere of Saturn has a peak electron concentration of* 2.3×10^4 *per cubic centimeter at an altitude of 2500 kilometers above the 1-bar level in the atmosphere, and a plasma scale height at the top of the ionosphere of 560 kilometers. Attenuation of monochromatic radiation at a wavelength of 3.6 centimeters propagating obliquely through Saturn's rings is consistent with traditional values for the normal optical depth of the rings, but the near-forward scattering of this radiation by the rings indicates effective scattering particles with larger than expected diameters of 10, 8, and 2 meters in the A ring, the outer Cassini division, and the C ring, respectively. Preliminary analysis of the radio tracking data yields new values for the masses of Rhea and Titan of* $4.4 \pm 0.3 \times 10^{-6}$ *and* $236.64 \pm 0.08 \times 10^{-6}$ *times the mass of Saturn. Corresponding values for the mean densities of these objects are* 1.33 ± 0.10 *and about 1.89 grams per cubic centimeter. The density of Rhea is consistent with a solar-composition mix of anhydrous rock and volatiles, while Titan is apparently enriched in silicates relative to the solar composition.*

Radio science observations of the Saturn system with Voyager 1 included (i) radio occultation measurements of the ionospheres and atmospheres of Titan and Saturn and of Saturn's rings and (ii) determination of the masses of satellites and the gravity field of Saturn based on radio tracking of the spacecraft. The relevant spacecraft and mission characteristics have been described (*1*). Results of other planned radio science investigations carried out with Voyager 1 will be reported later (*2*). In this report we give our present results for the atmosphere of Titan (*3*), the atmosphere and ionosphere of Saturn, the optical depth and particle sizes in Saturn's rings, and the masses of Rhea and Titan. The relative emphasis given these subjects reflects only our progress in making interpretations in each area.

The results given here are preliminary in that they are based on an incomplete data set (*4*)—essentially the observations available from the automatic systems employed for mission tracking, control, and data acquisition—and a preliminary orbit determination. Final reduction of the complete data set will lead to a much more detailed analysis. However, our substantive conclusions are not expected to change.

With the exceptions noted below, all radio propagation observations were carried out with the coherent dual-frequency radio system normally employed for telemetry and spacecraft tracking (*1*). The wavelengths were approximately 3.6 and 13 cm, but were in an exact 3:11 ratio. Antennas 64 m in diameter at NASA Deep Space Network tracking stations in Spain and Australia were used for data collection. Signal-to-noise ratios of approximately 10^5 and 10^4 were achieved at 3.6 and 13 cm, respectively, assuming a 1-second coherent integration time.

Atmosphere of Titan. The Voyager 1 trajectory near Titan was designed in part to optimize the radio occultation measurements of its atmosphere. However, because of the closeness of the encounter and the a priori uncertainties in the trajectory and in the size and orbital position of Titan, a strategy for pointing the spacecraft antenna at occultation entry and exit was needed to ensure good results if the atmosphere were tenuous and measurements to great depth if it were dense. Estimates of the surface pressure before the Voyager encounter ranged from a few tens of millibars to a few tens of bars; there were several suggestions for the main atmospheric constituents and a two-to-one range in predicted surface temperatures.

From the preliminary data, we conclude that the radio science experiment probed the atmosphere to the surface. Measured scale heights, in conjunction with other experimental and theoretical results, provide strong (albeit circumstantial) evidence that N_2 is the predominant atmospheric constituent. For pure N_2, preliminary indications are that the surface pressure and temperature at the near-equatorial position of occultation entry are 1.6 bars and 93 K, respectively, corresponding to an atmospheric density of 5.9 kg m^{-3}, or about 4.6 times that of dry air at standard temperature and pressure (STP).

Before occultation entry we offset the antenna boresight 0.11° from the direction to Earth in such a way that after this amount of refraction by the atmosphere the direction from the spacecraft to the virtual Earth would be along the boresight. This is the maximum offset that would allow complete amplitude and frequency measurements for the ionosphere and tenuous parts of the atmosphere of Titan. For atmospheric pressures of more than several hundred millibars, refraction would move the direction to the virtual Earth off-axis by an amount greater than the antenna beamwidth for the 3.6-cm wavelength. For pressures greater than 1 or 2 bars (depending on actual atmospheric conditions), the direction would fall outside the beamwidth for the 13-cm wavelength. In either case, the signal would be lost as a result of bending of the rays by the atmosphere, assuming they were not first intercepted by the surface of Titan. The spacecraft was behind Titan for about 10 minutes, and there was time for only one new antenna setting for occultation exit. We chose this to be 2.36° off-Earth, the maximum practical amount that would allow the 13-cm signal to be received after the spacecraft emerged from behind Titan. Although the 3.6-cm signals would be of limited use and most of the amplitude measurements at 13 cm would be imprecise, this larger offset would allow continuous and accurate frequency measurements at 13 cm over the maximum possible range in pressure.

The preliminary Doppler frequency data at 13 cm for occultation entry yield the temperature-pressure (T-p) profile shown in Fig. 1. The maximum indicated pressure is 1.6 bars, assuming 100 percent N_2. The profile terminates at this point since the weakening signal merged into the noise and the automatic radio

 0036-8075/81/0410-0201$01.25/0

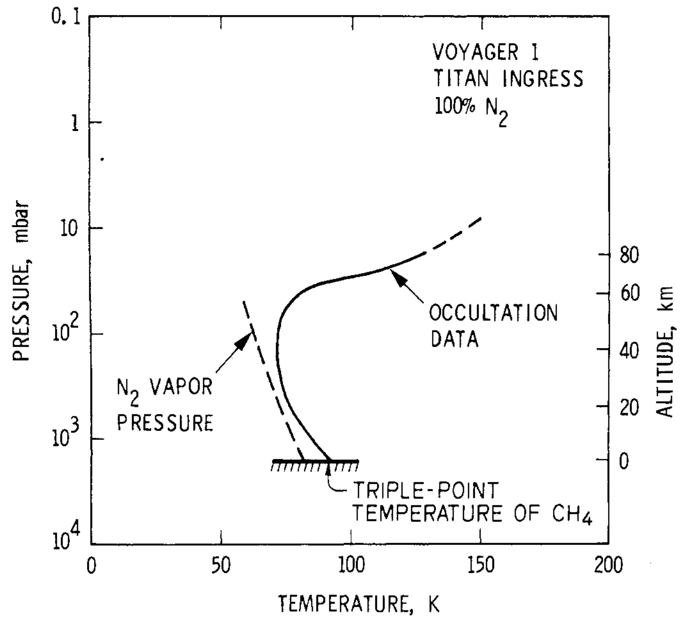

Fig. 1. Pressure-temperature-altitude relations for the equatorial atmosphere of Titan, assuming a pure N_2 atmosphere. The altitude scale is not linear. The N_2 vapor pressure curve and the methane triple-point temperature are shown for comparison.

receivers at the tracking station indicated "loss of lock" of the signal. As discussed above, this behavior was expected whether the surface pressure were about this value or some arbitrarily larger value.

A preliminary study of the high-rate 13-cm amplitude measurements for exit from occultation has made it possible to resolve the principal uncertainty about the location of the surface. It shows no signal at times when the exit conditions would correspond to larger bending angles than were measured at entry, even though the spacecraft antenna was then positioned to provide strong signals. However, at about the time when the exit conditions corresponded to the lowest measured entry altitude of Fig. 1, the signal suddenly rose to more than ten times the noise level. The nature of this reappearance is characteristic of rays just clearing a solid surface, and is uncharacteristic of either superrefraction or a change caused by an atmospheric absorbing layer. We see no reasonable alternative to the conclusion that the experiment probed atmospheric conditions to the surface of Titan.

From the approximate correspondence in bending angle for exit-signal start-up and entry-signal loss, it follows that the entry loss occurred for conditions certainly very near, and probably at, the surface. Thus in Fig. 1 we show temperature as a function of a (nonlinear) height scale as well as a logarithmic pressure scale. The zero reference altitude corresponds to a provisional radius for Titan of 2570 km (*5*). We emphasize that the indicated surface *T-p* values and the planetary radius are subject to possible future adjustments. However, we do not have such reservations about having reached the surface of Titan.

Figure 1 shows an approximate isotherm over several scale heights in the cold region of the middle atmosphere of Titan. The minimum measured scale height from the occultation experiment is about 16.4 km. This corresponds to a T/m ratio of 2.55 K per atomic mass unit, where m is mean molecular weight. At the indicated surface the scale height is about 20.6 km and $T/m \cong 3.32$. We plotted Fig. 1 on the basis of a pure N_2 atmosphere ($m = 28$) for the following reasons.

1) Of the atmospheric models proposed before the Voyager encounter, only those based on a preponderance of N_2 are compatible with the measured T/m ratios and the predicted temperatures (*6*). Constituents such as CH_4, NH_3, and CO_2, could neither exist alone nor predominate since they would not be gaseous at the corresponding temperatures.

2) The lowest indicated temperature at the longest wavelength measured by the Voyager IRIS experiment is 73 K, and the experimenters conclude that the minimum temperature in the atmosphere is about 70 K (*7*). This minimum corresponds to $m \cong 27.4$ when used with our radio results.

3) It appears that at some wavelengths IRIS measured to the surface and found a brightness temperature of 93 K (*7*). This would correspond to $m \cong 28$ if it applies with only minor modification to the near-surface atmosphere. The difference between the two derived m values is considered comparable to their uncertainties and therefore not significant. It is their proximity to the value for N_2 and not other proposed major constituents such as CH_4 and Ne that is important here (*6*).

4) The Voyager UVS experiment identified N, N_2, and N^+ in the upper atmosphere (*8*) and the IRIS experiment detected HCN (*7*), indicating that nitrogen is certainly present in the lower atmosphere of Titan.

5) Hunten (*6, 9*), following a suggestion of Lewis (*10*), proposed and modeled a predominantly N_2 atmosphere for Titan with the N_2 formed by conversion from an original inventory of ammonia. He used surface conditions of 20 bar and 200 K (*6*) but emphasized that the higher profile would be the same no matter where the surface was placed along his *T-p* curve. In fact, his model atmosphere is remarkably similar to Fig. 1 over the measured pressure range.

6) Atreya *et al.* (*11*) showed the photochemical steps in the evolution of a dense N_2 atmosphere for Titan. They proposed that early outgassing of ammonia and methane with subsequent production of H_2 by photolysis could produce a modest greenhouse effect, raising the temperature to the point where the ammonia would be irreversibly converted to nitrogen—and hydrogen, which mostly escapes—over the lifetime of the satellite.

Although $m \cong 28$ could, in principle, result from CO or mixtures of lighter and heavier gases, the combined experimental and theoretical evidence outlined above provides a persuasive case for the conclusion that the atmosphere of Titan is predominantly N_2.

Figure 1 includes the vapor pressure curve for N_2. It has a minimum separation from the derived profile of only a few degrees, so that, within the present uncertainties, we conclude that clouds consisting of liquid N_2 droplets might be present in the middle atmosphere.

Also illustrated in Fig. 1 is the triple-point temperature of methane, 90.7 K; the triple-point pressure is 117 mbar. Methane has long been known to be present in Titan's atmosphere and is probably the principal minor constituent (*6, 7*). Its presence will modify the given profile, which is based on pure N_2, but these changes are probably smaller than other current uncertainties. On the basis of the *T-p* structure in Fig. 1, clouds of solid frozen methane particles would be expected to form in the middle atmosphere if the methane abundance there exceeded ~ 1 percent by volume. Since measurements of the amount of methane above the cloud are consistent with this percentage (*7, 12*), they support this identification of the main dense cloud in the troposphere. For a higher methane abundance the cloud base would extend to lower altitudes, reaching the surface for the saturation abundance of about 7 percent. The cloud particles there might be liquid instead of solid methane since the surface temperature is approximately at the triple point. Note that measurements of the amount of methane above the cloud are not indicative of how much might lie below, just as measurements of the small water vapor content above high terrestrial clouds would not reveal the presence of a humid lower atmosphere over an ocean of water.

If C and N have their relative solar abundance in the present quantities of CH_4 and N_2 in the atmosphere and on the surface of Titan, then there is approximately 100 times more CH_4 on the surface than in the atmosphere, and one would expect rain and snow of liquid and solid methane onto surface methane at various locations on the satellite. The methane ocean or methane ice layer, if distributed over the surface, would be on the order of 1 km thick. If much of the original N remains in frozen ammonia, there might be even more surface methane. However, at least some of the atmospheric methane has been converted into larger molecules (*7*), so that the surface inventory of hydrocarbons probably includes more complex material, as suggested previously (*6*). It is also possible that Titan is relatively deficient in CH_4, as discussed by Prentice (*13*).

The close correspondence of the methane triple-point temperature and the apparent atmospheric temperature at the surface suggests a possible causal relationship, assuming there is a large surface inventory of both solid and liquid methane. That is, the global average temperature could not be much higher unless all of the surface methane were liquid, or much lower unless all of it were solid. In an analogous way, the average global temperature of the Earth is mediated by the H_2O interchange between the oceans and the polar ice caps and glaciers. Should there be a negative feedback mechanism for the temperature of Titan that involves a phase change in surface methane, Titan may have been locked near the present temperature for geologic times into the past, and destined to remain there far into the future. For example, photolysis dust particles might be lost to the temperature cycle when they fall on a liquid surface but not when they fall on a frozen surface. A cooling tendency would mean more solid surface and more dust both on the surface and raised by winds into the atmosphere, possibly resulting in more absorption of

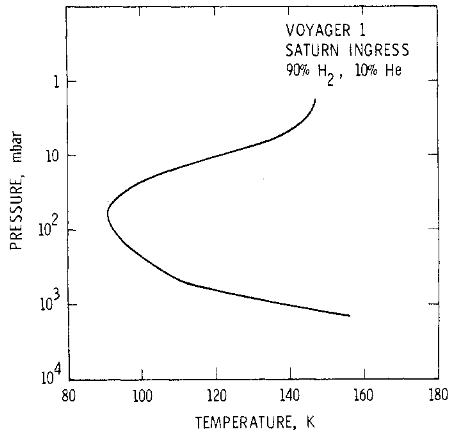

Fig. 2. Atmospheric temperature as a function of pressure for a south polar area of Saturn, assuming an atmosphere of 90 percent H_2 and 10 percent He by volume.

solar energy and hence a warming response. The hemispherical and polar difference seen in the Voyager 1 images (*14*) might be a seasonal effect of this type.

Earth's ancient atmosphere is believed to have been chemically reducing, and in some models it contained significant amounts of ammonia and methane, such as appears to have been the case for Titan. A fundamental difference in the subsequent evolution of the two atmospheres appears to have been that in addition to NH_3 and CH_4, liquid and gaseous H_2O played a central role on Earth in the developments that led to life and the present oxidizing atmosphere. On Titan, the temperature was too low for H_2O to participate in this way; instead, it constitutes about half the solid body of the satellite, as discussed below.

Atmosphere and ionosphere of Saturn. Entry occultation at Saturn was in the

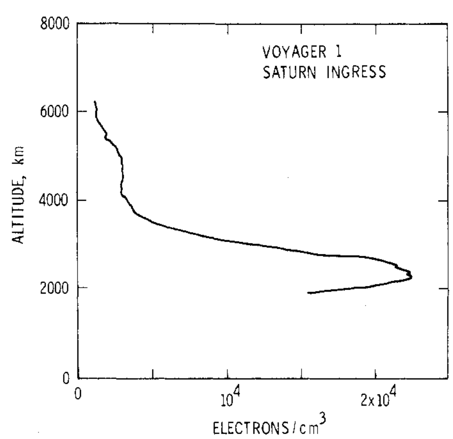

Fig. 3. Concentration of electrons as a function of altitude above the 1-bar level for the ionosphere of Saturn. Curve is for south polar latitudes near the evening terminator. The solar zenith angle was about 89°. The topside plasma scale height was about 560 km.

south polar region, with atmospheric measurements extending from 73.0 to 79.5°S over a longitude range of 14°. In deriving the *T-p* profile in Fig. 2, we assumed that the atmosphere is in hydrostatic equilibrium over this region. The profile is based on the preliminary data at both wavelengths. The 13-cm results extend to a pressure level of about 1.4 bar, where the temperature was 156 ± 10 K. For these results we assumed that the atmosphere consists of 90 percent H_2 and 10 percent He by volume (*15*). For other compositions the temperature is proportional to m, as explained for Titan. The pressure also depends on the assumed constituents, since its derived value is directly proportional to m and inversely proportional to the mean refractivity of the constituents at standard conditions.

The profile of Fig. 2 extends over a height range of about 200 km, displays an approximate adiabatic lapse rate in its lower region, and has a minimum tropopause temperature of about 91 K near 60 mbar. The temperature increases with altitude above the tropopause to about 150 K near 1 mbar.

It is not yet known if the maximum depth of penetration of these measurements was limited by the microwave absorbing properties of ammonia, as occurred for Jupiter at a pressure level of about 1 bar (*16*). More study of the data and comparison with other experiments will be required to investigate the amount of ammonia, the H_2-He mixing ratio, turbulence in the atmosphere, and possible changes in atmospheric structure with position on Saturn.

The ionosphere was also probed in the occultation experiment, and preliminary data for the entry location yield the profile of ionization shown in Fig. 3. The peak concentration of electrons in the measured range of heights is 2.3×10^4 cm^{-3} and occurs at an altitude of 2500 km above the 1-bar pressure level in the neutral atmosphere. The topside plasma scale height is about 560 km. While the polar location of this profile may be a controlling factor, the peak density is markedly lower than theoretical predictions and in this sense agrees with the Pioneer Saturn equatorial measurement (*15, 17*). However, the topside plasma scale height is markedly less than the corresponding interpretation of the Pioneer equatorial data. Additional Voyager 1 and Voyager 2 profiles will be important for further study of Saturn's ionosphere.

Saturn's rings. Voyager 1 emerged from behind Saturn at approximately 2°S, within the eastern ansa of the rings

Table 1. Normal optical depth τ, scattering gain G (α = 0), and particle size D_{equiv} in Saturn's rings. The range of optical depths shown gives the variation in the observed values; the scattering gain is with respect to a slab of isotropic particles with the same optical depth; the equivalent particle diameter is the approximate diameter consistent with the data for the case in which all particles are the same size. All values were derived from observations at 3.6 cm.

Feature	τ	G (α = 0)* (dB)	D_{equiv} (m)
A ring	0.65–0.80	25	10
Cassini division	0.15–0.65	34	8†
B ring	>1.0	?	?
C ring	0.02–0.28	30	2

*The scattering angle α is zero. †Near the A ring.

as seen from Earth. The spacecraft was then successively occulted by the C, B, and A rings, so that the radio path between the spacecraft and Earth was transected in order by these features. The received signals consisted of the attenuated energy propagating along the direct ray between Voyager 1 and Earth, and a second component scattered in the near-forward direction by particles within the extended beam of the spacecraft antenna (*18*). Thus the oblique optical depth of a point in the rings and the forward-scattering cross section of the surrounding region could be observed simultaneously. In addition, the Voyager 1 trajectory was chosen in part to produce a close alignment, within the region illuminated by Voyager 1, between the contours of constant received Doppler frequency and individual ringlets within the ring system (*19*), permitting ready mapping of the scattering phase function of any identifiable ring feature.

The preliminary data consist of a sequence of power-frequency spectra from the real-time monitor, which represent the region surrounding the received 3.6-cm wavelength data. These spectra have about 40 degrees of freedom and represent a few seconds of incoherent integration (*20*). The dynamic range of observation was about 40 dB for the direct signal, which could be identified as a coherent line in the monitor spectra.

We can measure simultaneously the attenuation of the direct signal and the strength of the near-forward–scattered energy during periods when the spacecraft was behind the A and C rings and the Cassini division. The attenuation of the B ring exceeds the dynamic range of the real-time monitor; neither direct nor scattered signal was detected for this feature (*21*). We can also identify and measure the near-forward–scattering phase function for the outer third of the Cassini division, based on the Doppler mapping mentioned above (*1, 22*).

Table 1 (*23*) presents estimates of the particle size in Saturn's rings from observations of the optical depth and scattering gain at the 3.6-cm wavelength. The values of particle size refer to the effective or "equivalent" scattering size, that is, the particle diameter in a monodisperse size distribution that would produce the combination of direct signal loss and forward-scattered power observed. The simplest model consistent with the 3.6-cm observation above is one in which all particles in each feature are the size given in Table 1. In the case of the Cassini division, the diffraction lobe of the scatter is apparent in the data (*24*); the width of this lobe is consistent with the size obtained from the combination of optical depth and scattering cross section. Note that our results for particle size apply only to limited regions of the rings and not to the system as a whole.

In Table 1, the optical depths of the A and C rings are in rough agreement with traditional values, but the optical depth of the Cassini division is larger than expected. The particle sizes are consistent with either a narrow distribution of large particles of about the size given, or a broad distribution of sizes such as might result from collisional processes (*25*). In either case, the 10-m size is larger than or at the upper limit of sizes usually stated in the observational literature.

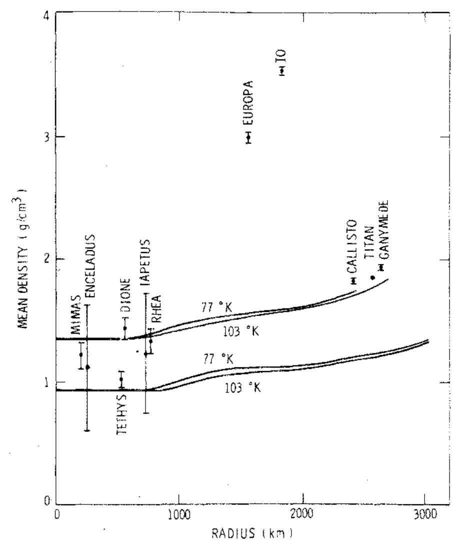

Fig. 4. Measured mean densities of some satellites of Saturn and the Galilean satellites of Jupiter as a function of radius. Mass uncertainties dominate the error bars for Enceladus, Rhea, and Iapetus. The lower curves correspond to models computed by Lupo and Lewis (*35*) for pure water-ice balls with isothermal temperatures of 77 and 103 K; the upper curves correspond to their isothermal models for satellites with a solar mix of 40 percent anhydrous chondritic rock and 60 percent water ice.

With regard to distributions of sizes inferred from radar observations, the contribution of each particle to the backscatter cross section is weighted as D^2, where D is the diameter, assumed to be larger than or comparable to $\lambda/3$, where λ is the wavelength. For forward scatter the weighting is D^4. Thus, for example, scattering particles with an inverse-cube-law size distribution would be inversely weighted with respect to size for scattering in the forward and back directions; the largest particles would contribute heavily to forward scatter, while the smallest particles would be most important in backscatter. Recent estimates of particles in the size range 2 to 200 cm based on radar backscatter and microwave emissions (*26*) are consistent with our results if one assumes a distribution similar to an inverse cube law.

Additional information about the particle size distribution is contained in the wavelength dependence of the optical depth and in the forward-scattering phase diagram of the ring particles. A

Table 2. Mass and related parameters for five satellites of Saturn and the two low-density Galilean satellites of Jupiter. The masses of Rhea and Titan and the radius of Titan are from this work. The masses of Mimas, Tethys, and Dione are from Kozai (*29*), the masses of Callisto and Ganymede from Null (*33*), and the radii of Callisto and Ganymede from Davies *et al.* (*34*). The interior parameters were computed for two-zone models with a core of anhydrous chondritic rock and an envelope of water ice.

Satellite	GM* (km^3 sec^{-2})	Radius (km)	Mean density (g cm^{-3})	Mass fraction of rock	Core radius (R_c/R)†
Mimas	2.50 ± 0.06	195 ± 5	1.21 ± 0.10	0.31	0.47
Tethys	41.5 ± 0.8	525 ± 10	1.03 ± 0.06	0.13	0.33
Dione	70.2 ± 2.2	560 ± 10	1.43 ± 0.09	0.47	0.57
Rhea	166 ± 10	765 ± 10	1.33 ± 0.10	0.37	0.51
Titan	8976 ± 3	2570 ± ?	1.89 ± ?	0.52	0.63
Callisto	7172 ± 24	2410 ± 10	1.83 ± 0.01	0.51	0.62
Ganymede	9885 ± 37	2638 ± 10	1.93 ± 0.01	0.54	0.64

*Here G is Newton's gravitational constant and M is mass. †Core radius divided by satellite radius.

thorough study of the particle size distribution must await the reduction of the complete ring occultation data set.

Gravity results. Preliminary least-squares solutions based on single-station Doppler tracking data from the Voyager 1 encounter with Saturn yield new information on the masses of Rhea and Titan. Other gravity parameters, such as the masses of other satellites, gravitational spherical harmonics for Saturn, and the total mass in the rings, are not improved, but inclusion of multiple-station and other data types in the solutions should provide additional information about these parameters.

The solutions give masses of $4.4 \pm 0.3 \times 10^{-6}$ M_S for Rhea and $236.64 \pm 0.08 \times 10^{-6}$ M_S for Titan, where M_S is the mass of Saturn. The mass of Rhea is consistent with values previously determined from satellite dynamics and the Pioneer 11 flyby (*27–31*), and about a factor of 3 times more accurate than the best previous results. Similarly, the mass of Titan is about a factor of 3 times more accurate than the Pioneer 11 result, and is consistent with less accurate earlier results from satellite dynamics (*32*).

We used the new values for the masses of Rhea and Titan, the radio occultation radius of Titan (*5*), and preliminary radii for other satellites from the Voyager imaging team (*14*) to compute mean densities for a number of satellites of Saturn. These densities are shown in Fig. 4, where we include the Galilean satellites of Jupiter for reference. The values of mass for Mimas, Enceladus, Tethys, and Dione were from Kozai (*29*), the values for the Galilean satellites from the Pioneer 10 and Pioneer 11 Jupiter flybys (*33*), and the radii of the Galilean satellites from the Voyager imaging results at Jupiter (*34*). The densities of these objects are compared with theoretical curves for satellites consisting of pure water ice and alternatively of 60 percent water ice and 40 percent anhydrous chondritic rock by mass (*35*). We find that the mean densities of Mimas, Dione, and Rhea are roughtly consistent with the 60:40 mix of ice and rock; the densities of Enceladus and Iapetus are not sufficiently well determined to distinguish between the two alternatives given. Tethys appears to be roughly consistent with water ice, but we caution that its density will be much better determined after the Voyager 2 encounter. We also find that the mean densities of Callisto, Titan, and Ganymede are remarkably similar and slightly greater than expected on the basis of theoretical curves for satellites of roughly solar composition.

We computed the percentage of rock by mass, the radius of the rock core, and the average moment of inertia for each satellite for which new Voyager 1 data provided reasonably accurate mean densities. We assumed that the satellites consist of totally differentiated anhydrous chondritic rock and water ice, and used spherical models with uncompressed rock cores of 3.66 g cm^{-3} and ice envelopes of 0.932 g cm^{-3}. Next, we accounted for compressional and thermal corrections to the zero-order models by interpolating between models published by Lupo and Lewis (*35*). Compressional effects are not important for Mimas, Tethys, and Dione, but compression of the ice in Rhea increases the mean density of the envelope more than 3 percent. In the larger satellites—Titan, Callisto, and Ganymede—the mean density of the envelope is increased by roughly 30 percent and that of the rock core by 7 percent. Results of these computations are given in Table 2.

On the basis of these approximate interior models, we conclude that Titan and Callisto have a bulk composition of about 52 percent rock by mass, with perhaps a slightly higher value for Ganymede. This composition is probably not affected appreciably by reasonable assumptions about the relative distribution of rock and ice, as long as the rock remains anhydrous. Therefore the composition of the large satellites is probably enhanced in rock with respect to the solar mix. Perhaps evolutionary effects, including the heat from internal differentiation and compaction at formation, caused a loss of volatiles in all three large satellites.

Note added in proof: The strong forward-scattering region mentioned in association with the Cassini division is located 121,000 km from the center of Saturn. Whether this location is within the Cassini division or the inner edge of the A ring is subject to the final definition of these features.

G. L. TYLER
V. R. ESHLEMAN
Center for Radar Astronomy, Stanford University, Stanford, California 94305
J. D. ANDERSON
G. S. LEVY
G. F. LINDAL
G. E. WOOD
Jet Propulsion Laboratory, California Institute of Technology, Pasadena 91103
T. A. CROFT
Radio Physics Laboratory, SRI International, Menlo Park, California 94025

References and Notes

1. V. R. Eshleman, G. L. Tyler, J. D. Anderson, G. Fjeldbo, G. S. Levy, G. E. Wood, T. A. Croft, *Space Sci. Rev.* **21**, 207 (1977).
2. The other investigations include measurements of the gravitational redshift of the spacecraft oscillator associated with the Saturnian potential well, studies of turbulence in the ionosphere and atmosphere of Saturn and possibly Titan from occultation data, studies of the plasma distribution in the Saturnian magnetosphere from dual-frequency tracking data, and studies of the mean size and size distribution of particles in Saturn's rings from microwave measurements of near-forward scatter.
3. We present no results for the ionosphere of Titan; the preliminary data were lost as a result of a brief failure of the real-time data system. Occultation data for Titan's ionosphere were recorded by a separate system and will be reduced at a future date [see (*4*)].
4. The primary data set for radio propagation and scattering observations consists of high-time-resolution recordings of the radio signals received at the tracking stations. These recordings preserve amplitude, frequency, phase, and polarization. Transcription of this data set to computer-compatible electronic format is in progress at the time of this writing. The results here are based on (i) automatic measurements of signal frequency, amplitude, and spectrum, and (ii) preliminary examination of the signal amplitudes from the high-rate data for Titan occultation. The characteristic parameters of the automatic equipment, such as the time constant of response, are fixed during observation and cannot be modified after the fact, whereas the processing of the raw data recordings can be optimized for each signal parameter of interest over the dynamic conditions of the event. The results based on the high-rate recordings from the station are superior in signal-to-noise ratio and, usually, time resolution to the automatic machine results. In addition, the occultation results depend on accurate knowledge of the spacecraft trajectory, which is still subject to revision by the Voyager navigation team. Much more detailed results can be expected in the future, particularly with regard to the occultation investigations.
5. The value of 2570 km is based on the average value of entry and exit occultation radii, where the entry value is obtained from a complete inversion of frequency data for the atmosphere profile and the exit value is based on estimates derived from exit amplitude data only. The entry and exit radii used differ by 10 to 50 km, depending on the orbit solution employed. We believe 2570 km to be near the correct value but cannot determine the uncertainties at this time. Our final value will be based on complete inversion of data from both entrance and exit occultation events. Our preliminary value for the radius based on occultation entrance only was 2560 km. Note that changes in the value of the radius affect our conclusions regarding the mean density of Titan, and that the residual errors in the orbit indicated by the differing entry and exit radii imply the presence of small residual errors in the occultation *T-p* profile.
6. D. M. Hunten, Ed., *NASA Spec. Pub. 340* (1974); D. M. Hunten and D. Morrison, Eds., *NASA Conf. Publ. 2068* (1978).
7. R. Hanel *et al.*, *Science* **212**, 193 (1981).
8. A. L. Broadfoot *et al*, *ibid.*, p. 206.
9. D. M. Hunten, *J. Atmos. Sci.* **30**, 726 (1973).
10. J. S. Lewis, *Icarus* **15**, 174 (1971).
11. S. K. Atreya, T. M. Donahue, W. R. Kuhn, *Science* **201**, 611 (1978).
12. L. M. Trafton, *Astrophys. J.* **175**, 295 (1972); K. Rages and J. B. Pollack, *Icarus* **41**, 119 (1980).
13. This deficiency could arise if Titan condensed from solar nebular gases at a temperature above the condensation point of CH_4 clathrate but below that of NH_3 hydrate. See A. J. R. Prentice, *JPL Publ. 80-80* (1980); in *The Origin of the Solar System*, S. F. Dermott, Ed. (Wiley, London, 1978), p. 111.
14. B. A. Smith *et al*, *Science* **212**, 163 (1981).
15. A. P. Ingersoll, G. S. Orten, G. Münch, G. Neugebauer, S. C. Chase, *ibid.* **207**, 439 (1980); A. J. Kliore, G. F. Lindal, I. R. Patel, D. N. Sweetnam, H. B. Hotz, T. R. McDonough, *ibid.*, p. 446.
16. G. F. Lindal *et al.*, *J. Geophys. Res.*, in press.
17. M. B. McElroy, *Space Sci. Rev.* **14**, 460 (1973); S. K. Atreya and T. M. Donahue, *Icarus* **24**, 358 (1975); *ibid.* **25**, 335 (1975); J. H. Waite, Jr., thesis, University of Michigan (1981).
18. The half-power width of the Voyager antenna is approximately 0.8° and 3° at 3.6 and 13 cm, respectively. The ring area illuminated at 3.6 cm is an oval about 3,000 by 30,000 km in size.

19. The differential Doppler shift F_D of a signal received on Earth after scattering by a ring particle is measured with respect to the directly propagating signal. Loci of constant F_D form contours of constant Doppler shift in the ring plane. The Voyager 1 trajectory was chosen to align these Doppler contours with coordinates of constant radius within the ring plane to the extent possible. An osculating condition between the Doppler contours and the azimuthal ring coordinate was achieved within the area illuminated by the spacecraft antenna, so there is a strong mapping between the Doppler shift of the received signals and radial ring position (*1*).
20. Integration times were changed in the course of the experiment from about 6 to about 3 seconds; precise values are not available for this system. The standard deviation of a single smoothed spectrum is estimated to be slightly greater than 0.5 dB or 10 percent, which is consistent with the other parameters of the system.
21. The nominal value of the optical depth of the B ring, estimated from previous Earth-based observations, is in the range 1 to 1.5 measured perpendicular to the ring plane. At Voyager 1 encounter the obliquity of the ring plane relative to the Voyager-Earth line was 6.1°, so that the effective optical depth along the ray path is about one order of magnitude greater than the normal optical depth. Consequently, the estimated attenuation along the radio path is in the range 40 to 60 dB, assuming the ring particles are all large with respect to the microwave wavelengths employed. Processing of the data recordings from the tracking station (*4*) should permit detection and measurement of the direct signal attenuation in this range.
22. E. A. Marouf, thesis, Stanford University, Stanford, Calif. (1975).
23. Optical depth is obtained directly from the reduction in direct signal intensity measured in spectra from the real-time monitoring system. The values given represent averages over radial extents of several hundred kilometers in the ring plane. Particle scattering gain is calculated from the intensity of the forward-scattered radiation relative to the noise and the known parameters of the signal path. This gain is relative to a slab of isotropic scatterers of the same optical depth. E. A. Marouf has calculated parametric curves for the exact forward-scattering cross section as a function of optical depth over a range of monodispersive size distributions. These curves are appropriate to the Voyager geometry and include multiple scatter. For the monodispersive case, the optical depth and scattering cross-section yield a unique solution for particle size. Marouf assumed a cloudlike distribution of particles surrounding the mean ring plane. If future results indicate that the particles lie essentially in a monolayer, the particle sizes must be recalculated.
24. Forward scattering from the outer third of the Cassini division is approximately 6 dB stronger than that from the adjacent inner portion of the Cassini division or the A ring. Variations in the strength of this feature as the direct ray approached and then passed through the Cassini division can be mapped to yield the forward-scattering phase function of particles. The half-power width of the scattering lobe is approximately 0.25° at 3.6 cm, implying a particle size for a monodispersive distribution of about 8 m.
25. H. Alfvén and G. Arrhenius, *NASA Spec. Publ. SP-345* (1976).
26. J. N. Cuzzi and J. B. Pollack, *Icarus* **33**, 233 (1978); E. E. Epstein, M. A. Janssen, J. N. Cuzzi, W. G. Fogarty, J. Mottmann, *ibid.* **41**, 103 (1980). J. N. Cuzzi, J. B. Pollack, A. L. Summers, manuscript "Saturn's rings: Particle composition and size distribution as constrained by observations at microwave wavelengths II," Radio Interferometric Observations (1980).
27. H. Jeffreys (*28*) gives a value for the mass of Rhea of $3.2 \pm 3.8 \times 10^{-6}$ M_S, Y. Kozai (*29*) gives $9.0 \pm 2.6 \times 10^{-6}$ M_S, and W. I. McLaughlin and T. D. Talbot [*Mon. Not. R. Astron. Soc.* **179**, 619 (1977)] give $4.8 \pm 0.8 \times 10^{-6}$ M_S; all are based on orbital precessions in the Saturn satellite system. J. D. Anderson *et al.* (*30*) give $3.8 \pm 1.3 \times 10^{-6}$ M_S, and G. W. Null *et al.* (*31*) give $4.0 \pm 0.9 \times 10^{-6}$ M_S, both from the Pioneer 11 flyby.
28. H. Jeffreys, *Mon. Not. R. Astron. Soc.* **114**, 433 (1954).
29. Y. Kozai, *Publ. Astron. Soc. Jpn.* **28**, 675 (1976).
30. J. D. Anderson, G. W. Null, E. D. Biller, S. K. Wong, W. B. Hubbard, J. J. MacFarlane, *Science* **207**, 449 (1980).
31. G. W. Null, E. L. Lau, E. D. Biller, J. D. Anderson, *Astron. J.*, in press.
32. W. S. Eichelberger [*Publ. U.S. Nav. Obs.* 6 (1911), appendix 2B, p. 1] gives $239.7 \pm 4.9 \times 10^{-6}$ M_S for the mass of Titan from a numerical integration of the orbit of Hyperion. H. Jeffreys (*28*) gives $241.2 \pm 1.8 \times 10^{-6}$ M_S from perturbations on Iapetus; J. D. Anderson *et al.* (*30*) give $237.0 \pm 2.7 \times 10^{-6}$ M_S from the Pioneer flyby; G. W. Null *et al.* (*31*) give $238.8 \pm 3.0 \times 10^{-6}$ M_S from a combined analysis of Pioneer 11 and satellite dynamics data. P. J. Message [*Trans. Int. Astron. Union* **10**, 111 (1958)] gives a high value of $246.22 \pm 0.13 \times 10^{-6}$ M_S from perturbations on Hyperion. However, Message later [in *Dynamics of the Solar System*, R. L. Duncombe, Ed. (Reidel, Dordrecht, Netherlands, 1979), p. 159] discussed errors in the satellite theory for Hyperion and difficulties in deriving a mass for Titan from the theory. The numerical integration of Eichelberger avoids these difficulties.
33. G. W. Null, *Astron. J.* **81**, 1153 (1976).
34. M. E. Davies, T. A. Hauge, F. Y. Katayama, J. A. Roth, *Rand Corp. Rep. R-2532-JPL/NASA* (1979).
35. M. J. Lupo and J. S. Lewis, *Icarus* **40**, 157 (1979).
36. We thank the members of the Voyager Project operations teams and the Deep Space Network for their support in acquisition of the radio science data. We thank the Voyager navigation team, in particular J. K. Campbell, R. A. Jacobson, and S. P. Synnott, for making available their preliminary fits to the two-way Doppler and optical navigation data and the Voyager imaging team for prepublication values of radii. We also thank A. J. R. Prentice for numerous discussions and assistance in the interpretation of the mean densities of the satellites of Saturn. We especially thank B. J. Buckles, P. E. Doms, D. F. Finnerty, and D. P. Holmes for their efforts in the implementation and execution of these experiments and H. B. Hotz and D. N. Sweetnam for their help in the profile computation. E. A. Marouf has played a vital role over many years in the concept, development, design, implementation, and analysis of the ring occultation experiment and we gratefully acknowledge his contribution. This work was supported by the National Aeronautics and Space Administration.

9 February 1981

Extreme Ultraviolet Observations from Voyager 1 Encounter with Saturn

Abstract. *The global hydrogen Lyman α, helium (584 angstroms), and molecular hydrogen band emissions from Saturn are qualitatively similar to those of Jupiter, but the Saturn observations emphasize that the H_2 band excitation mechanism is closely related to the solar flux. Auroras occur near 80° latitude, suggesting Earth-like magnetotail activity, quite different from the dominant Io plasma torus mechanism at Jupiter. No ion emissions have been detected from the magnetosphere of Saturn, but the rings have a hydrogen atmosphere; atomic hydrogen is also present in a torus between 8 and 25 Saturn radii. Nitrogen emission excited by particles has been detected in the Titan dayglow and bright limb scans. Enhancement of the nitrogen emission is observed in the region of interaction between Titan's atmosphere and the corotating plasma in Saturn's plasmasphere. No particle-excited emission has been detected from the dark atmosphere of Titan. The absorption profile of the atmosphere determined by the solar occultation experiment, combined with constraints from the dayglow observations and temperature information, indicate that N_2 is the dominant species. A double layer structure has been detected above Titan's limb. One of the layers may be related to visible layers in the images of Titan.*

Saturn's atmosphere. Saturn's upper atmosphere is qualitatively similar to Jupiter's, consisting mainly of H, H_2, and He above a layer of ultraviolet (UV)-absorbing hydrocarbons. These constituents are measured in emission and absorption by the Voyager ultraviolet spectrometer (UVS) (*1*).

Hydrogen Lyman α (Ly α) emission arises from resonance scattering of the solar line at 1216 Å and by particle excitation. The disk-averaged Ly α brightness of Saturn measured from rocket and Earth-orbital experiments ranges from 0.7 kR (kilorayleigh) (*2, 3*) to 1.5 kR (*4*). The Voyager UVS found a central-disk brightness of 3.3 kR, which corresponds to a disk-averaged brightness of 1.5 kR if the brightness varies as a cosine function from center to limb. A few hundreds of rayleighs of this emission may arise in the H atmosphere of the rings. The implied H column abundance on Saturn is about 5×10^{16} cm^{-2}, somewhat less than the abundance of 1×10^{17} to 3×10^{17} cm^{-2} at Jupiter (*1*). Helium (584 Å) emission is scattered from the strong solar line at that wavelength. The measured central-disk intensity is 2.2 ± 0.3 R, but a substantial part of this may arise in the extended region out to 25 Saturn radii (R_S).

As at Jupiter, the Lyman and Werner bands of H_2 are also radiated from the dayside disk. Figure 1 compares spectra from the central regions of Saturn and Jupiter taken under similar conditions. The intensity integrated over the H_2 Lyman and Werner bands is about 0.7 kR, or about 25 percent of the intensity at Jupiter. This factor of 4 is nearly the same as the factor of 3.3 reduction in solar flux from Jupiter to Saturn. The general structure of the Jupiter and Saturn spectra between 900 and 1700 Å is similar, although there are differences between 1100 and 1200 Å and in the region near 1570 Å (Fig. 1).

Emissions from the dark atmosphere of Saturn at Ly α (0.35 kR) and He (584